Cryogenic Relaxation Oscillators Enabled by Isostructural Insulator-Metal Transition in Strain-Engineered VO_2 Thin-Film Devices

Ehsan Ansari[1], Fabio Bersano[1], Pascal Alexander Schouwink[2], Adrian Mihai Ionescu[1]
[1]Nanoelectronic Device Laboratory, EPFL, 1015, Lausanne, Switzerland
[2]X-Ray Diffraction and Surface Analytics Platform, EPFL, 1951, Sion, Switzerland
Email: ehsan.ansari@epfl.ch, adrian.ionescu@epfl.ch

Abstract*—Cryogenic neuromorphic computing, oscillatory and spiking neural networks, and emerging quantum systems require low-power oscillators that remain operational at deep cryogenic temperatures. In this study, we demonstrate the first cryogenic relaxation oscillator based on vanadium oxide by fabricating strain-engineered vanadium dioxide (VO_2) thin-film devices. The low-power oscillator is tunable, operates from just below 230 K down to 7 K, reaches frequencies up to 3.8 MHz, and exhibits power consumption below 75 µW, with further improvement expected through device scaling, suggesting potential compatibility with millikelvin cryogenic platforms. The enabling material is a 50 nm strained VO_2 film that undergoes an isostructural insulator-metal transition (IMT), enabling a predominantly electronic transition without the usual structural phase transition. This is achieved by pinning the monoclinic (M1) phase across the transition through strain engineering. Raman spectroscopy and grazing-incidence X-ray diffraction confirm a metallic M1 phase at room temperature and indicate compressive strain, unlike conventional VO_2 films, which adopt a metallic rutile (R) phase above their transition temperature. Electrical measurements show a reduced transition temperature of about 230 K, compared with about 340 K in relaxed films. Fabricated two-terminal strained VO_2 devices exhibit hysteresis and negative differential resistance across cryogenic temperatures down to 7 K, enabling cryogenic relaxation oscillator operation and low-temperature switching applications.

Keywords—VO_2, cryogenic relaxation oscillator, strain engineering, isostructural insulator-metal transition

I. Introduction

Cryogenic electronic circuits are attracting increasing interest for superconducting electronics, cryo-CMOS interfaces, quantum computing, ultra-low-noise sensing, space systems, and cryogenic neuromorphic hardware. In these platforms, compact low-power oscillators are essential for timing, signal generation, oscillatory neural networks (ONNs), spiking neural networks (SNNs), and hybrid quantum-classical interfaces.

In parallel, emerging functional materials are attracting attention for beyond-CMOS devices. Among them, correlated oxides exhibiting an insulator-metal transition (IMT) are promising switching elements for compact and energy-efficient oscillatory circuits. Vanadium dioxide (VO_2), which exhibits an IMT and a structural phase transition (SPT) near 67 °C [1], has been widely studied as a two-terminal switching element for relaxation oscillators and oscillatory neural networks [2], [3], [4], [5]. However, while cryogenic operation has been explored in threshold-switching oxides such as NbO_2 and HfO_2-based devices, comparable cryogenic oscillator operation based on VO_2 has remained unexplored [6]. This is because conventional VO_2-based oscillators are inherently limited to operation near room temperature (RT), where the electrically triggered IMT typically involves an electronic (Mott) transition closely coupled with a structural (Peierls) phase transition from the monoclinic (M1) phase to the rutile (R) phase (Fig. 1)[9]. This thermally driven process involves a significant energy barrier, increasing device stress and affecting reliability [10]. While conventional VO_2 devices operate at RT, at cryogenic temperatures, we observe that they undergo electrical breakdown before IMT switching, rendering them unsuitable for reliable cryogenic operation.

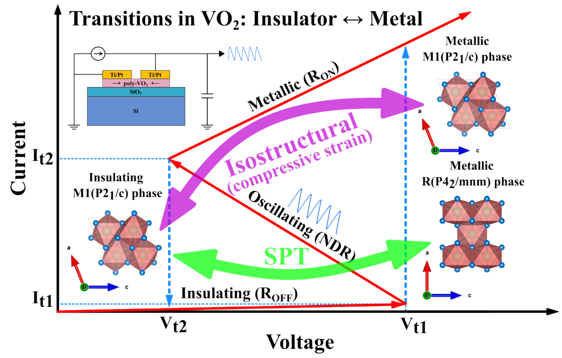

Fig. 1. Conceptual illustration of electrical switching, phase evolution, and relaxation oscillator operation in VO_2 two-terminal devices. The I-V characteristics show the insulating (OFF), oscillatory negative differential resistance (NDR), and metallic (ON) regimes. The structural schematics compare the conventional M1-to-R phase transition with the isostructural transition in this work, where the M1 phase remains pinned across the IMT. A schematic of the VO_2 device and oscillator is also shown. Crystal structures are obtained from Materials Project (mp-1102963 and mp-19094) and visualized using VESTA [7], [8].

In this work, we overcome this limitations using strain-engineered polycrystalline VO_2 thin films that enable an isostructural, predominantly electronic (Mott) transition. Structural pinning of the M1 phase is achieved through a tailored rapid thermal processing (RTP) of atomic layer deposited (ALD) films, which introduces compressive strain, suppresses the SPT, and reduces the transition temperature to approximately 230 K, thereby facilitating IMT switching at cryogenic temperatures (Fig. 1). Grazing index X-ray diffraction (GIXRD) and Raman spectroscopy are employed to confirm M1-phase pinning. Based on this approach, we demonstrate the first cryogenic relaxation oscillator based on vanadium oxide, operating from below 230 K down to 7 K. The oscillator performance is characterized down to 7 K, highlighting the potential of strain-engineered VO_2 IMT devices for cryogenic clock generation, oscillatory circuits, and neuromorphic applications.

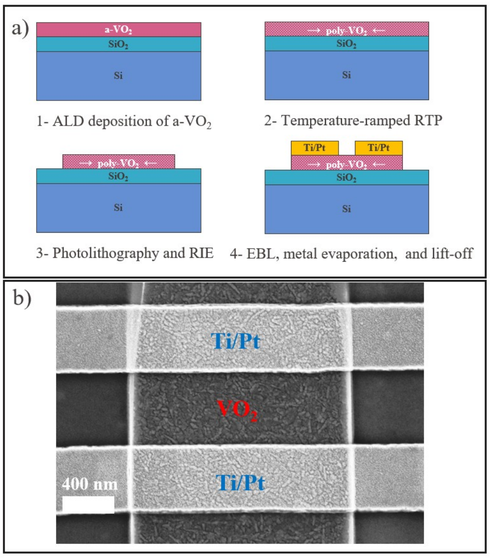

Fig. 2. a) Process flow of device fabrication; arrows in the poly-VO_2 thin film represent the compressive strain b) SEM image of the fabricated two-terminal VO_2 device after ~10^9 oscillation cycles, showing nanoscale grain structure.

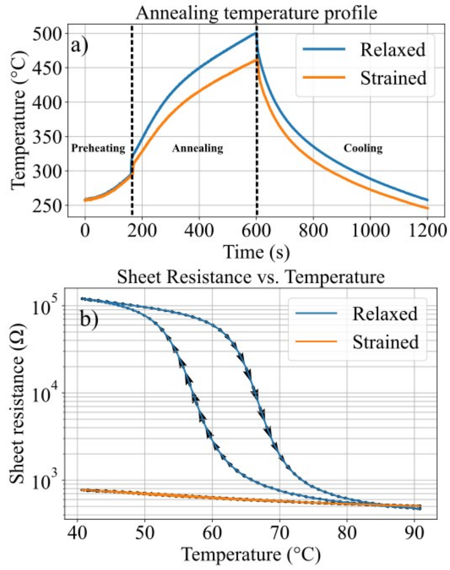

Fig. 3. a) Annealing temperature profiles for the strained sample (38% power) and the relaxed sample (42% power). b) Sheet resistance versus temperature for both samples after annealing, measured above RT.

II. Materials and Methods

A. Device Fabrication

The fabrication process of two-terminal VO_2 devices begins with the deposition of a 50 nm amorphous VO_2 (a-VO_2) thin film on a 100 nm SiO_2 layer grown on a silicon substrate. The film is deposited by ALD with tetrakis(ethylmethylamino)vanadium (TEMAV) and water (H_2O) as precursors, similar to those used in [11]. Post-deposition annealing is performed using a constant-power, temperature-ramped (RTP) system, which enables by our novel method both crystallization and strain engineering of the polycrystalline VO_2 (poly-VO_2) thin films. The devices are then defined using photolithography followed by reactive ion etching (RIE). Subsequently, Ti (5 nm)/Pt (50 nm) metallic contacts are patterned using electron-beam lithography (EBL) and lift-off, with metal deposition carried out by electron-beam evaporation. Fig. 2 shows the fabrication process flow and scanning electron microscope image (SEM) of the device fabricated and used in cryogenic relaxation oscillators.

B. VO_2 Thin Film Strain Engineering

Typically, VO_2 undergoes a thermally driven IMT at temperatures around 340 K. This transition is accompanied by an SPT from the low-temperature insulating monoclinic (M1) phase to the high-temperature metallic rutile (R) phase (Fig. 1) [1]. Some reports suggest that under electrical excitation, VO_2 undergoes the IMT just prior to the SPT, with both transitions remaining tightly coupled [9]. However, isostructural IMT has also been reported in strained VO_2 thin films [10]. In particular, strain can induce a metallic monoclinic phase at room temperature due to bandgap narrowing, which remains pinned during the electrically triggered IMT, enabling a predominantly electronic (Mott) transition without an accompanying SPT. Furthermore, compressive strain along the c-axis has been shown to reduce the transition temperature down to near RT [12], [13]. In this work, we demonstrate that a temperature-ramped RTP introduces sufficient compressive strain in the polycrystalline VO_2 film during crystallization of the amorphous ALD layer to not only lower the IMT temperature to approximately 230 K, but also stabilize a metallic M1 phase at RT, indicating suppression of the SPT (Fig. 1).

We employ a fast and facile three-step annealing process using a constant-power-controlled RTP system. The process consists of (i) a preheating step at 32% power for 3 min, (ii) an annealing step at 38% power for 7 min, and (iii) a cooling step at 10% power for 10 min. Finally, the power is reduced to zero, allowing the sample to cool naturally to RT. The RTP is carried out in an oxygen ambient at 0.1 mbar.

Fig. 3a depicts the resulting temperature profile measured by a pyrometer positioned near the substrate. The profile exhibits a ramp-up and ramp-down behavior, with a maximum temperature of 461 °C for the strained sample. By adjusting the power during the annealing step while keeping the duration constant, the induced strain in the film, its IMT temperature, and its room-temperature (RT) conductivity can be controlled. When a higher power setpoint of 42% is used, corresponding to a maximum temperature of around 500 °C, the strain in the film is relaxed. This behavior may be attributed to increased plasticity of the film at elevated temperatures and is consistently observed at higher power setpoints. The sheet resistance as a function of temperature for both relaxed and strained samples is measured using a four-point probe system in a temperature-controlled chamber above RT, as shown in Fig. 3b. The relaxed sample exhibits an IMT at approximately 67 °C, consistent with typical VO_2 films, whereas the strained sample remains in a highly conductive metallic state without a thermally induced IMT. However, subsequent cryogenic and low-temperature measurements at the device level reveal that the strained sample undergoes an IMT at temperatures around 230 K (−43 °C).

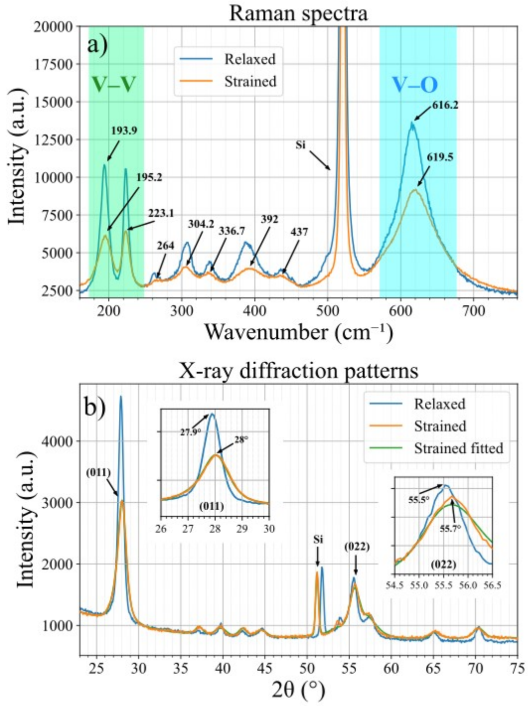

Fig. 4. a) Raman spectra and b) GIXRD patterns of the relaxed and strained samples measured at RT. Rietveld refinement fitting is shown in green. The inset provides a zoom-in of the main M1 phase peaks.

C. *Structural Characterization*

Structural analysis is performed using Raman spectroscopy with a 532 nm excitation laser at RT. Both relaxed and strained samples are analyzed and compared, as shown in Fig. 4a. While a typical VO_2 film in the metallic state exhibits the R phase, the Raman spectra of the strained metallic sample show clear M1 phase peaks, consistent with previous reports [9], [14], indicating that the M1 structure remains dominant. This confirms the structural pinning of the M1 phase in the metallic state. Additionally, the Raman peaks corresponding to V–O and V–V bond vibrations are blue-shifted (from 616.2 to 619.5 cm^{-1} and 193.9 to 195.2 cm^{-1}, respectively) in the strained sample relative to the relaxed sample, consistent with compressive strain-induced lattice stiffening and reduced bond lengths in the polycrystalline film, where the measured shifts reflect an averaged response over multiple grains.

Further structural analysis is performed using GIXRD on both samples at RT. The diffraction peaks are consistent with previous reports [14], indicating a dominant M1 phase. Rietveld refinement of the strained sample shows good fit with the measured data, further confirming M1-phase pinning in the metallic state at RT and the presence of compressive strain. Consistent with Raman analysis, the two main XRD peaks corresponding to M1 (011) and (022) planes are shifted to higher angles relative to the relaxed sample, which can be attributed to compressive strain in these directions (Fig. 4b).

Based on this analysis, we confirm the structural pinning of the VO_2 M1 phase in the strained sample in its electrical metallic state, along with the presence of effective compressive strain.

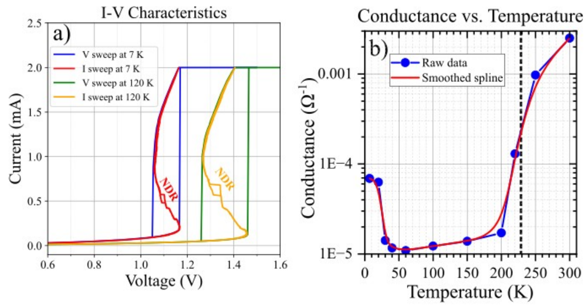

Fig. 5. a) I-V characteristics of a two-terminal strained VO_2 device (similar to Fig. 2b) measured at 7 and 120 K exhibiting NDR and hysteresis. b) Temperature dependence of the device conductance under cryogenic conditions.

III. Device Cryogenic Electrical Characteristics

Cryogenic electrical measurements are performed using a SUSS MicroTec PMC 150 cryogenic probe station in conjunction with a Keithley 4200A semiconductor parameter analyzer. Fig. 5a shows the I-V characteristics of a two-terminal strained VO_2 device (similar to Fig. 2b) measured at 7 K and 120 K in vacuum (5×10^{-6} mbar). The voltage (V) sweep cycles performed with a current compliance of 2 mA (blue and green curves) exhibit clear hysteresis loops, while the current sweep measurements (red and yellow curves) reveal negative differential resistance (NDR) regions between the threshold voltages, both of which are essential for relaxation oscillator operation. These characteristics are consistent with the conceptual illustration shown in Fig. 1. It should be noted that the I-V curves in the NDR regime appears noisy and less accurate, as the device undergoes oscillations at ~500 kHz due to coupling with the current source output capacitance and parasitic cable capacitances.

To further characterize the device, the conductance of the device is measured over a temperature range from 7 K to 300 K (see Fig. 5b). A transition temperature of ~230 K is observed. In addition, the conductance increases with increasing temperature in the range from ~50 K to 300 K. We also observe that the IMT threshold voltage (V_{t1}) increases as the temperature decreases from ~230 K to ~50 K. These trends are similar to those reported for conventional VO_2 devices, typically near 340 K [15]. Consistently, in devices fabricated from relaxed VO_2 films, we observe V_{t1} increases as the temperature is reduced from room temperature. However, below ~250 K, the V_{t1} becomes sufficiently large that these devices undergo electrical breakdown before reaching the IMT, rendering them unsuitable for reliable low-temperature operation. In contrast, strained devices exhibit increased conductance (Fig. 5b) and a reduction in the V_{t1} when cooling from ~50 K down to 7 K. This behavior contrasts with previous reports and is consistent with a predominantly electronic Mott-type IMT, where the collapse of the insulating state is governed mainly by electronic correlations rather than lattice transformation.

IV. Cryogenic VO_2 Relaxation Oscillator

Relaxation oscillator circuits are implemented based on the schematic shown in the inset of Fig. 6 using the device shown in Fig. 2b. To decouple the device from the current source output capacitance and parasitic cable capacitances,

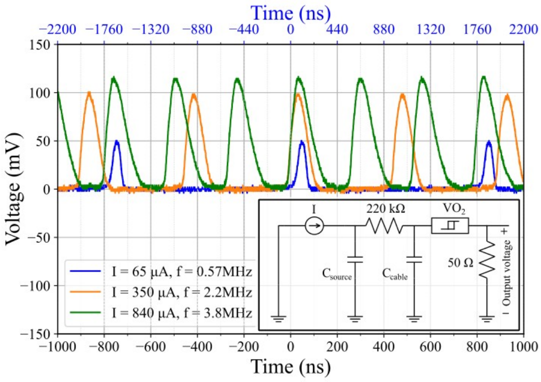

Fig. 6. Oscillator output voltage measured across a 50 Ω resistor at 7 K, showing frequencies of 3.8, 2.2, and 0.57 MHz for bias currents of 840, 350, and 65 µA, respectively. The top axis corresponds to the blue curve. The inset shows the schematic of the implemented oscillator circuit.

and to suppress the resulting undesired oscillations, a 220 kΩ series resistor is inserted between the source and the VO_2 device. To minimize parasitic cable capacitance, a short coaxial cable is used between the series resistor and the VO_2 device inside the cryogenic probe station; however, an estimated parasitic capacitance of ~15 pF remains in the circuit. Direct connection of an oscilloscope to the VO_2 device inside the cryogenic chamber introduces additional capacitive loading, which can disturb the oscillator operation. Therefore, the oscillatory signal is measured indirectly by monitoring the device current through the voltage drop across a 50 Ω series resistor placed outside the cryogenic chamber using an oscilloscope. Fig. 6 shows the oscillation signals at 3.8, 2.2, and 0.57 MHz, obtained by applying bias currents (I) of 840, 350, and 65 µA to the device at 7 K, respectively. Based on the measured V_{t1} of 1.16 V, the upper-bound estimate of the oscillator's power consumption (P), calculated as $P = V_{t1} \times I$, yields 974, 406, and 75 µW, respectively. This demonstrates the tunability of the oscillator via current control. The device dimensions are W = 1.7 µm and L = 570 nm, with potential for further scaling. Scaling the VO_2 device, along with reducing the parasitic capacitance in the circuit, is known to lower power consumption to sub 10 microwatt range and increase operating frequencies toward ~100 MHz [4], [16]. These measurements demonstrate the functionality of strain-engineered VO_2 devices for cryogenic oscillatory and switching operations over a wide temperature range, from below 230 K down to 7 K, with potential for further extension toward millikelvin regimes.

V. Conclusion

We demonstrate strain-engineered VO_2 thin films exhibiting an isostructural IMT, enabled by M1-phase pinning. Structural characterization confirms the dominant M1 phase and compressive strain, supporting a predominantly electronic (Mott) transition. Electrical measurements show a reduced transition temperature (~230 K) and stable switching down to 7 K. Unlike relaxed VO_2 devices, strained films operate reliably from ~230 K to 7 K. We further demonstrate the first cryogenic VO_2-based relaxation oscillator, operating at up to 3.8 MHz with power consumption down to below 75 µW. These results highlight strain engineering as an effective approach for low-power cryogenic VO_2 oscillators and switching devices, with potential applications in clock generation, oscillatory circuits, neuromorphic computing, cryo-CMOS interfaces, quantum systems, space electronics, and low-temperature sensing.

Acknowledgment

The authors acknowledge the Center of Micro Nano Technology (CMi) of EPFL and all colleagues of Nanolab involved in the ALD process development under SWIMS ERC Synergy. This work is funded by the Swiss National Science Foundation (SNSF) under Grant No. 208233.

References

[1] S. Biermann, A. Poteryaev, A. I. Lichtenstein, and A. Georges, "Dynamical Singlets and Correlation-Assisted Peierls Transition in VO_2," *Phys. Rev. Lett.*, vol. 94, no. 2, p. 026404, Jan. 2005, doi: 10.1103/PhysRevLett.94.026404.

[2] E. Corti, B. Gotsmann, K. Moselund, A. M. Ionescu, J. Robertson, and S. Karg, "Scaled resistively-coupled VO_2 oscillators for neuromorphic computing," *Solid-State Electronics*, vol. 168, p. 107729, Jun. 2020, doi: 10.1016/j.sse.2019.107729.

[3] W. Yi, K. K. Tsang, S. K. Lam, X. Bai, J. A. Crowell, and E. A. Flores, "Biological plausibility and stochasticity in scalable VO_2 active memristor neurons," *Nat Commun*, vol. 9, no. 1, p. 4661, Nov. 2018, doi: 10.1038/s41467-018-07052-w.

[4] Z. Pollner *et al.*, "VO_2 Oscillator Circuits Optimized for Ultrafast, 100 MHz-Range Operation," *Advanced Electronic Materials*, vol. n/a, no. n/a, p. e00433, doi: 10.1002/aelm.202500433.

[5] F. Bersano *et al.*, "Monolithically Integrated VO_2 Mott Oscillators for Energy-Efficient Spiking Neurons," 2026, *arXiv*. doi: 10.48550/ARXIV.2604.21487.

[6] M. M. Islam, S. Alam, M. S. Hossain, K. Roy, and A. Aziz, "A review of cryogenic neuromorphic hardware," *J. Appl. Phys.*, vol. 133, no. 7, p. 070701, Feb. 2023, doi: 10.1063/5.0133515.

[7] A. Jain *et al.*, "Commentary: The Materials Project: A materials genome approach to accelerating materials innovation," *APL Mater.*, vol. 1, no. 1, p. 011002, Jul. 2013, doi: 10.1063/1.4812323.

[8] K. Momma and F. Izumi, "VESTA 3 for three-dimensional visualization of crystal, volumetric and morphology data," *J Appl Cryst*, vol. 44, no. 6, pp. 1272–1276, Dec. 2011, doi: 10.1107/S0021889811038970.

[9] H.-T. Kim *et al.*, "Raman study of electric-field-induced first-order metal-insulator transition in VO_2-based devices," *Appl. Phys. Lett.*, vol. 86, no. 24, Jun. 2005, doi: 10.1063/1.1941478.

[10] A. Moatti, R. Sachan, V. R. Cooper, and J. Narayan, "Electrical Transition in Isostructural VO_2 Thin-Film Heterostructures," *Sci Rep*, vol. 9, no. 1, Feb. 2019, doi: 10.1038/s41598-019-39529-z.

[11] A. Varini *et al.*, "Pulsed Laser and Atomic Layer Deposition of CMOS-Compatible Vanadium Dioxide: Enabling Ultrathin Phase-Change Films," *ACS Appl. Electron. Mater.*, Jul. 2025, doi: 10.1021/acsaelm.5c01132.

[12] Y. Muraoka and Z. Hiroi, "Metal–insulator transition of VO_2 thin films grown on TiO_2 (001) and (110) substrates," *Appl. Phys. Lett.*, vol. 80, no. 4, Jan. 2002, doi: 10.1063/1.1446215.

[13] J. Cao *et al.*, "Strain engineering and one-dimensional organization of metal–insulator domains in single-crystal vanadium dioxide beams," *Nature Nanotech*, vol. 4, no. 11, pp. 732–737, Nov. 2009, doi: 10.1038/nnano.2009.266.

[14] V. V. Strelchuk *et al.*, "Effect of structural disorder on the modification of V–V and V–O bond lengths at the metal-dielectric phase transition in VO_2 thin films," *Materials Science in Semiconductor Processing*, vol. 174, p. 108224, May 2024, doi: 10.1016/j.mssp.2024.108224.

[15] L. Pósa *et al.*, "Interplay of Thermal and Electronic Effects in the Mott Transition of Nanosized VO_2 Phase Change Memory Devices," *ACS Appl. Nano Mater.*, vol. 6, no. 11, pp. 9137–9147, Jun. 2023, doi: 10.1021/acsanm.3c00150.

[16] S. Dutta, A. Khanna, W. Chakraborty, J. Gomez, S. Joshi, and S. Datta, "Spoken vowel classification using synchronization of phase transition nano-oscillators," in *2019 Symposium on VLSI Technology*, Jun. 2019, pp. T128–T129. doi: 10.23919/VLSIT.2019.8776534.